JOURNAL OF MATERIALS SCIENCE 13 (1978) 985–996

# The cyclic creep behaviour of Type 316 stainless steel

D. G. MORRIS, D. R. HARRIES
*Metallurgy Division, AERE, Harwell, UK*

The cyclic creep behaviour of a Type 316 stainless steel at 625° C has been examined as a function of the maximum applied stress and frequency using trapezoidal loading cycling between zero and a maximum stress. The so-called "static-to-dynamic creep transition" observed is interpreted in terms of recoverable anelastic strain behaviour without using an internal stress argument. Over the range of experimental conditions examined, failure occurs by static creep modes, namely wedge crack nucleation and growth. The loading strain increments appear to be damaging to about the same extent as the much slower strain occurring at constant load, such that it is the overall strain rate that determines the rate of damage. A cursory examination of square wave load cycling shows that the behaviour is very similar to that observed during trapezoidal loading and suggests that the rate of loading and unloading does not play an important part in determining the creep and rupture behaviour.

## 1. Introduction

Many studies have been carried out to examine the influence of cyclic loading (from zero load to a maximum load) on elevated temperature creep deformation, and both acceleration and deceleration relative to the static creep rate has been observed [1]. At low frequencies (less than one cycle per hour) static creep behaviour is approximated [1]. However, for frequencies in the range 0.1 to $10^3$ $min^{-1}$ much lower creep rates are often observed [2–6]. Such behaviour appears perfectly general and has been observed in a wide range of single phase metals and alloys (of fcc, bcc and cph structures) and precipitation-hardened alloys including austenitic stainless steels and nickel based alloys (see for example [4]); the only instances in which slower creep is not generally observed has been in tests on very high purity metals [4]. An acceleration in the creep rate occurs at higher frequencies when the fatigue influence becomes dominant [7].

The reduced creep rate produced by the "static-to-dynamic" transition has been attributed to precipitation hardening [5], a stress rate yielding effect [7, 8], and, more recently, to an internal stress-produced creep recovery [2–4]. The latter argument involves the reversed movement of dislocations during the low load period under the action of a very high internal stress. It has been suggested, however, that a similar retrograde dislocation movement under the action of high internal stress leads to the weakening of dislocation barriers such that enhanced creep occurs on subsequent reloading [9–11]; this latter argument has been used to explain the cyclic enhancement of creep rate sometimes observed at low temperatures for a series of single phase metals and low alloy steels [11–14]. The operating mechanisms and the balance between cyclic strengthening and weakening appear, therefore, to be poorly understood and in need of further examination.

Cyclic creep fracture is a phenomenon that has received comparatively little study. In some cases (e.g. [15]) slow frequency load or temperature cycling produces only slight changes in the rupture behaviour. Nevertheless, when structural changes are brought about by thermal ageing [15, 16] or when relatively large numbers of cycles are imposed before fracture, very dramatic changes in creep fracture properties have been

observed [15–17]. Furthermore, it has been shown that the cycle details can play an important part in determining behaviour. For example, Harrison and Tilly [18] noted that a rectangular loading cycle hardly affects the rupture properties of a cast nickel alloy, whilst a triangular loading cycle leads to a significant increase in the rupture life. Ellison and Walton [19] reported a reduction in rupture life on load cycling a low alloy steel and related this to an enhanced creep crack growth rate: it was suggested that the enhancement occurs during reloading to the higher load value such that the creep behaviour is very dependent on the frequency and rate of loading.

It follows from the above brief review that a number of mechanisms may be operative during cyclic creep, leading to significant beneficial or detrimental changes in the creep and rupture properties. The present study was, therefore, carried out in an attempt to isolate the operative mechanism(s) in the cyclic creep of a Type 316 austenitic stainless steel at 625° C.

## 2. Experimental details

The details of the material and specimen geometry have been described in a previous report [20]. The cyclic creep tests were carried out at 625° C on a 50 kN capacity servotest hydraulic machine with the specimen enclosed in a muffle furnace, using heated testing arms to achieve a temperature stability and spatial variation of less than 0.5° C. Extension measurements were made using a pair of Linear Variable Differential Transducers attached to the ends of the specimen gauge length by means of stainless steel rods. Comparative creep and rupture testing has been carried out previously using the same batch of Type 316 steel and the results detailed [21, 22]. Load cycling was carried out by applying trapezoidal load cycles with the load cycled from zero to $L_{max}$. For each

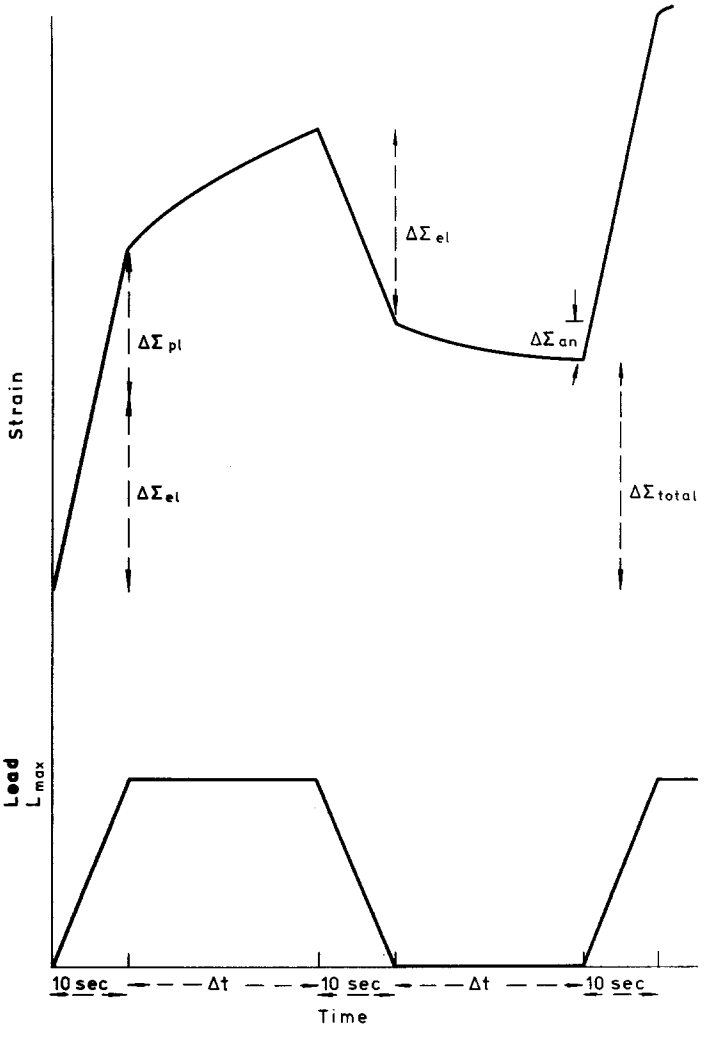


*Figure 1* A single creep cycle illustrated schematically.

cycle the load and unload times ($\Delta t$) were equal and a wide range of $\Delta t$ values was examined. The load cycle is illustrated schematically in Fig. 1, together with an illustration of a typical material response. The time taken to load (and unload) was 10 sec, independent of the testing frequency. The cyclic creep tests were carried out using load-hold times ranging from 5 sec to 1 week and stresses from 290 to 200 MPa, producing rupture lives in the range 10 to 1000 hours. In addition, several tests were carried out using square wave load cycling (analogous to trapezoidal cycling with loading and unloading times of $10^{-3}$ sec). The ranges of applied stresses and frequencies were similar to those in the trapezoidal load cycling tests.

The influence of cyclic loading on the extent of anelastic strain was examined in specimens crept at constant load to the mid-secondary creep stage; several measurements of the recoverable anelastic strain were made on each specimen by re-imposing several load cycles on specimens crept under a static load for several hours. In addition, after cycling for a given period, the load was held constant and the transition to static creep observed.

Optical metallographic examinations, using standard sectioning and preparation procedures, were made on the gauge lengths of fractured specimens to determine the extent of the internal creep damage. The details of the dislocation microstructure corresponding to the various cyclic creep tests were examined by transmission electron microscopy, again using conventional specimen thinning procedures.

## 3. Results

### 3.1. Typical cyclic creep behaviour

The typical creep strain–time plot (Fig. 1.) showed an instantaneous elastic strain increment, $\Delta\epsilon_{el}$, produced a loading, equivalent to that on unloading, and a plastic strain increment, $\Delta\epsilon_{pl}$. During the maximum load period the initially high creep rate decreased progressively to a relatively constant value at longer times. Creep rates described later in this paper usually refer to the total unrecoverable strain per cycle ($\Delta\epsilon_{total}$) divided by the maximum load time ($\Delta t$), or, if specifically referred to, the total creep strain per cycle with the plastic loading effects removed (i.e. $\Delta\epsilon_{total} - \Delta\epsilon_{pl}$) divided by the maximum load time. Some anelastic strain, $\Delta\epsilon_{an}$, was recovered during the unload period.

All the parameters associated with the creep cycling were strongly dependent on the maximum load or stress and the testing frequency. Fig. 2 shows the accummulation of creep strain with total time at maximum load; the tests were carried out at different frequencies at a constant maximum load, corresponding to an initial stress of 250 MPa, the number of cycles to failure being given by $t_f/\Delta t$ (listed in Table I). For very slow cycling ($\Delta t = 6$ h, 1 h, 6 min), large loading increments, $\Delta\epsilon_{pl}$, were observed leading to a

TABLE I Creep and rupture data obtained from static and cyclic creep testing at 625° C. Both creep rates and rupture lives relate to time at maximum load during cycling.

| Testing mode | Applied stress (MPa) | Creep rate ($sec^{-1}$) | | Rupture life (time on load) (h) | Ductility (%) | Cycles to failure |
|---|---|---|---|---|---|---|
| Static | 290 | $3 \times 10^{-6}$ | | 17 | 55 | 1 |
| | 250 | $6.5 \times 10^{-7}$ | | 70 | 60 | 1 |
| | 230 | $2.5 \times 10^{-7}$ | | 150 | 60 | 1 |
| | 200 | $7 \times 10^{-8}$ | | 750 | 70 | 1 |
| Cyclic with hold period | | | | | | |
| 30 sec | 290 | $2.5 \times 10^{-6}$ | $3 \times 10^{-7}$ | 24 | 65 | 2 900 |
| 6 h | 250 | $10 \times 10^{-7}$ | $8 \times 10^{-7}$ | 65 | 80 | 11 |
| 1 h | 250 | $12 \times 10^{-7}$ | $7 \times 10^{-7}$ | 47 | 70 | 47 |
| 6 min | 250 | $12 \times 10^{-7}$ | $1.5 \times 10^{-7}$ | 55 | 70 | 550 |
| 30 sec | 250 | $2.6 \times 10^{-7}$ | $3 \times 10^{-8}$ | 150 | 70 | 18 000 |
| 5 sec | 250 | $2 \times 10^{-7}$ | very small | 200 | 70 | 144 000 |
| 6 min | 230 | $2.6 \times 10^{-7}$ | $4 \times 10^{-8}$ | 200 | 65 | 2 000 |
| 30 sec | 230 | $6 \times 10^{-8}$ | $6 \times 10^{-9}$ | 700 | 70 | 84 000 |
| 168 h | 200 | $6.5 \times 10^{-8}$ | $6 \times 10^{-8}$ | 830 | 70 | 5 |
| 24 h | 200 | $6.5 \times 10^{-8}$ | $6 \times 10^{-8}$ | 850 | 70 | 35 |

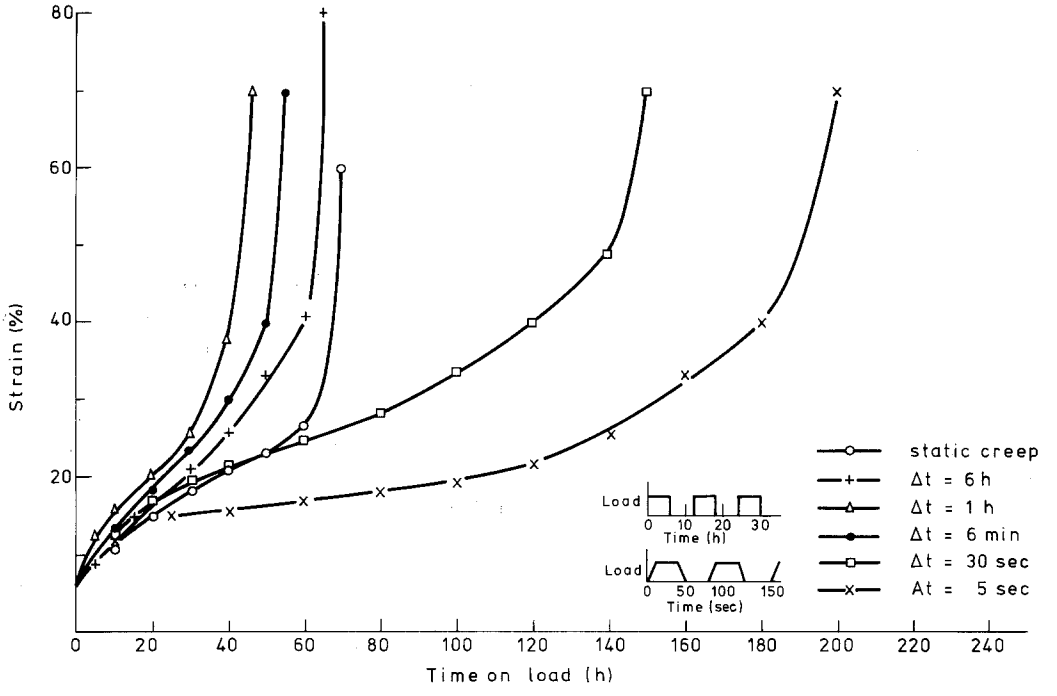


*Figure 2* Static and cyclic creep at an initial stress of 250 MPa at 625° C. The cyclic creep tests were carried out using a trapezoidal cycle with a constant time loading/unloading of 10 sec. The duration of the hold periods, $\Delta t$, are indicated. The cyclic creep data has been plotted as a function of time at maximum load. Load cycles have been indicated schematically for two of the tests.

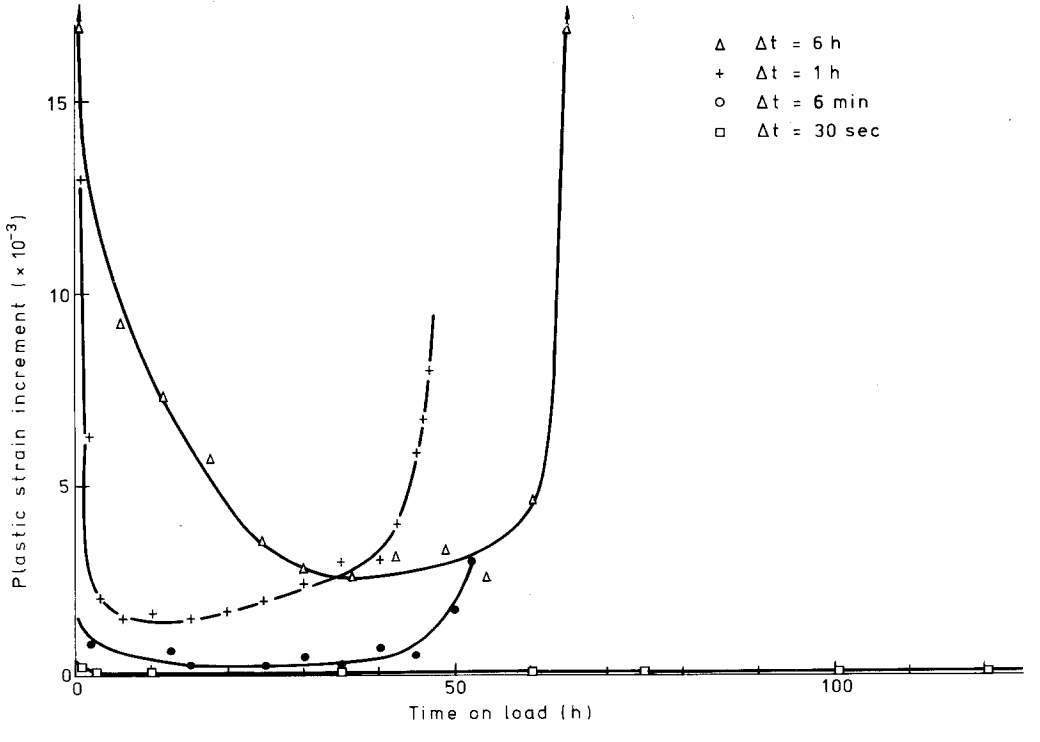


*Figure 3* Loading increments during cyclic creep at an initial stress of 250 MPa at 625° C.

rapid accummulation of strain and shorter rupture lives. However, with faster cycling ($\Delta t = 30$ sec, 5 sec) the loading increments became very small and the rate of strain accummulation decreased as the so-called static-to-dynamic transition occurred. Long rupture times resulted.

## 3.2. Loading increments

The magnitudes of the plastic loading increments, $\Delta\epsilon_{pl}$, were dependent not only on the maximum stress and cyclic frequency but also on the stage of the creep test at which the load cycling was carried out; this is illustrated in Fig. 3 for specimens cycled to rupture at differing frequencies. In general, the loading increments decreased during primary creep, achieved minimum values during secondary creep, and increased prior to failure. The rate of hardening was considerably greater and the minimum value of the plastic increment was much smaller, for the fast than for the slow cycling; this is evident from a comparison of the results of the tests with $\Delta t = 30$ sec and 6 h.

Despite this indication of material hardening induced by cycling, there was no evidence of any associated structural changes. For example, one specimen was cycled with $t = 6$ min to achieve the minimum plastic loading increment and the loading increments were subsequently measured after unloading for times ranging from 20 sec to 1 h. The loading increments were similar to the minimum values shown in Fig. 3 for the same unload time; this indicates that the plastic loading increments were dependent only on the duration of the unload period and that the cyclic loading, *per se*, had no effect on dislocation microstructure.

This conclusion was supported by transmission electron microscope observations showing no significant changes in the dislocation microstructure as a result of cycling. The only noticeable change was an apparent slight decrease in the dislocation density as a result of unloading for several hours (e.g. a dislocation density of $3 \times 10^{14}$ m$^{-2}$ reducing to $2.5 \times 10^{14}$ m$^{-2}$ after 10 h unload time at 625° C). Reloading after the unload period led to an increase in the dislocation density to the original value so that there was no cycle dependent change.

## 3.3. Creep rates and rupture behaviour

A significant proportion of the total creep deformation in a cycle occurred on loading, as is evident from the results in Table I, where the creep rates, both including and excluding the plastic loading increments (that is $\Delta\epsilon_{total}/\Delta t$ and $(\Delta\epsilon_{total} - \Delta\epsilon_{pl})/t$), are recorded. Fig. 4 illustrates

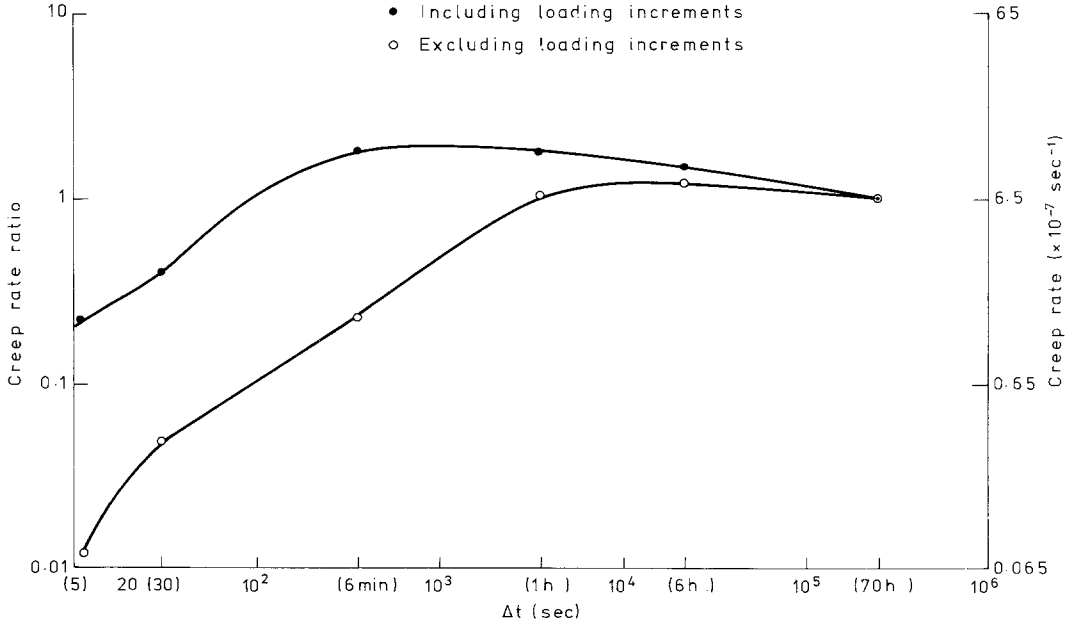


*Figure 4* Creep rates as a function of cyclic frequency (duration of hold periods, $\Delta t$). Tests conducted at an initial stress of 250 MPa at 625° C. The creep rate ratio, $\dot{\epsilon}_{cc}/\dot{\epsilon}_{sc}$ has been plotted, where $\dot{\epsilon}_{cc}$ is the cyclic creep rate at a given frequency and $\dot{\epsilon}_{sc}$ the static creep rate for the same applied stress and temperature.

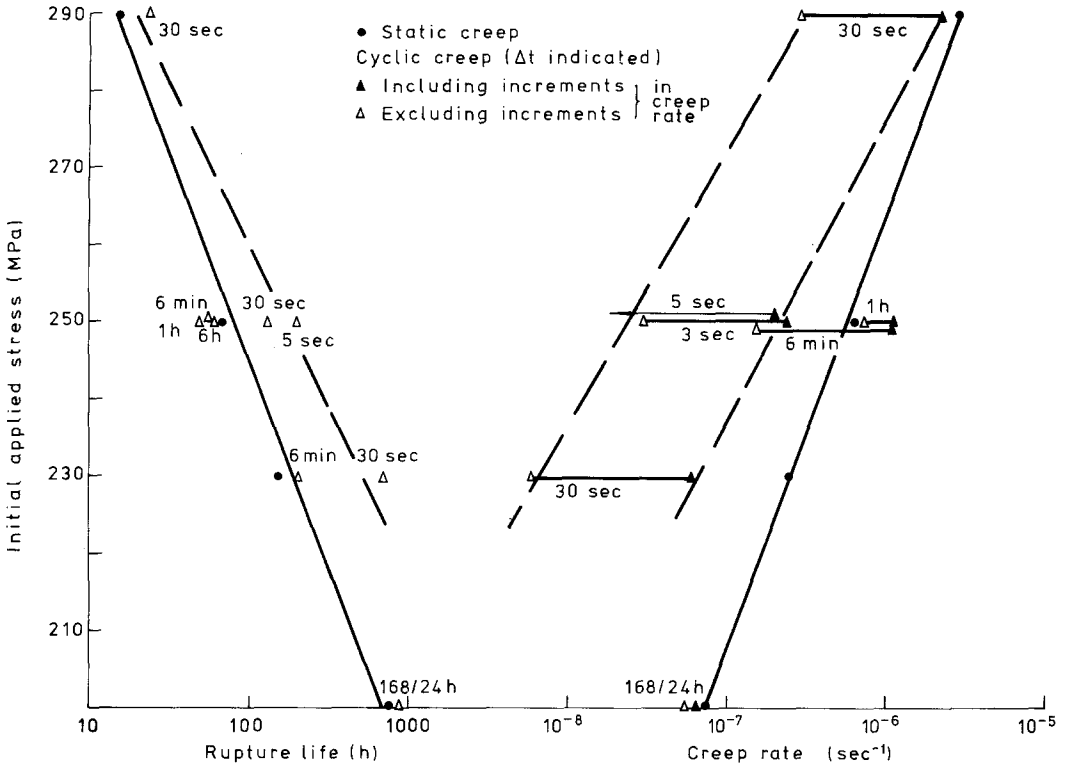


*Figure 5* Creep rates and rupture lives (time on-load to failure) as a function of applied stress for static and cyclic creep.

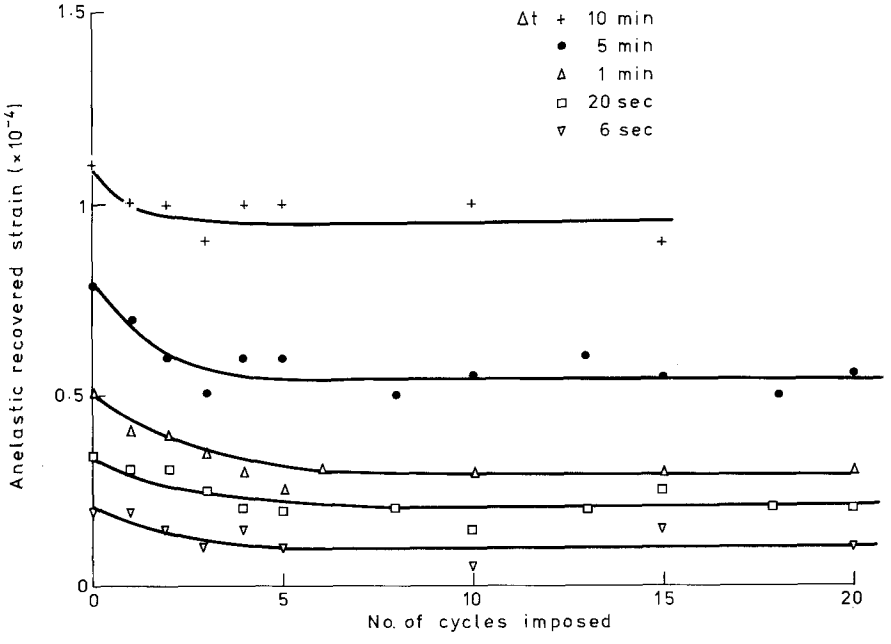


*Figure 6* The amount of recovered anelastic strain observed during load-off periods on commencing load cycling. The initial state corresponds to that of a specimen crept under a static load at an inititial stress of 250 MPa to the steady state stage.

the effect of testing frequency on these two measures of creep rate. The creep rates have been related to the static creep rate at the same stress, as was done by Koteragawa and Shimohata [2], and both increases and decreases in creep rates are evident. The increased creep rates for the slow cycling relative to static creep testing were due entirely to the loading strain, while for the fast cycling the creep rates were very low as both plastic loading increments and subsequent creep rates became very small.

Creep rates and rupture lives for those specimens taken to failure are plotted in Fig. 5 and listed in Table I for each of the applied loads and cycle frequencies examined. Both measures of cyclic creep rates have been indicated in Fig. 5 with the pairs of creep rate data linked; continuous lines have been drawn through the static creep data and dashed lines through the cyclic creep data for $\Delta t = 30$ sec. The changes in rupture life (maximum load time to failure) correlate with the changes in the creep rate (including plastic loading increments) for each load and frequency; that is, decreases in creep rate led to increases in rupture life and vice versa. The effect of cyclic loading on rupture strain was not dramatic for the range of cyclic tests examined, see Table I. There appeared to be a slight increase in ductility during trapezoidal cycling but this change was small and comparable to the scatter in the ductility data.

### 3.4. Anelastic strain during cyclic creep

The influence of cyclic loading on the anelastic strain recovery during the unload period is shown in Fig. 6. The magnitude of the recoverable anelastic strain depended not only on the period but also on the number of load cycles after the initial static creep period. Thus, the anelastic strain recovery during any load-off period decreased from the initial value, corresponding to recovery of the static creep dislocation structure, and reached an equilibrium value within about five cycles. The smaller anelastic recovery observed during shorter load-off periods is consistent with the previously examined time dependency of anelastic strain recovery [21], which indicated that approximately 1000 sec were required to recover all the anelastic strain. For very slow cycling, the extent of the recovered anelastic strain was approximately constant and equal to the total recovered anelastic strain in a static creep test.

### 3.5. Re-imposition of static load after cyclic loading

On reloading after a load-off period there were immediate elastic and plastic loading strains, as

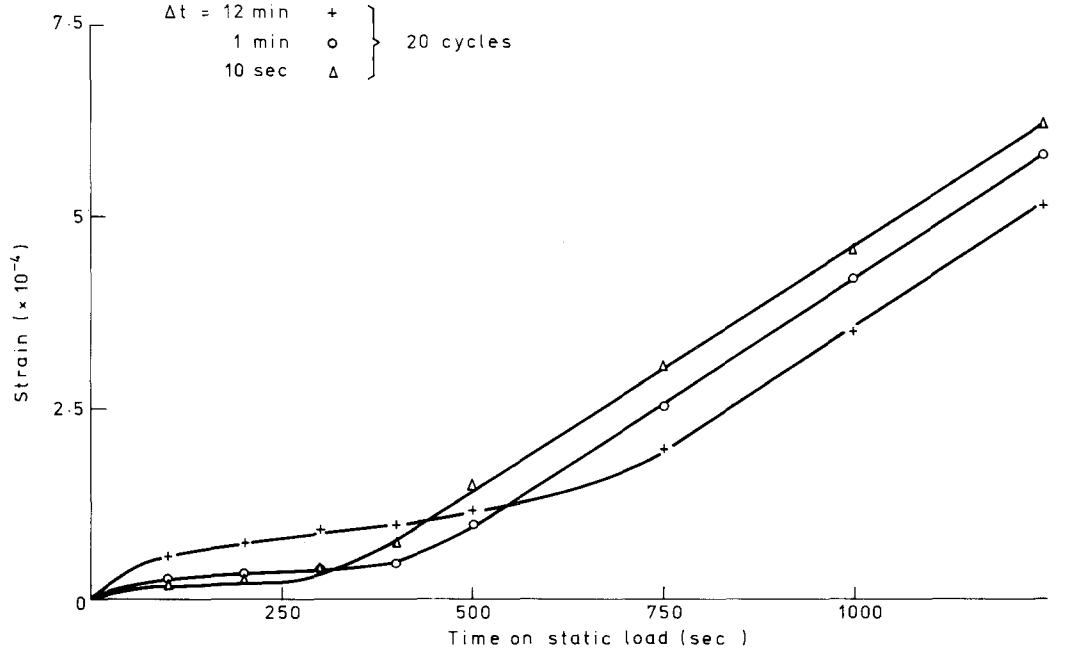


*Figure 7* Creep behaviour on imposing a static load after cyclically loading at the indicated frequency. Load corresponds to an initial stress of 250 MPa.

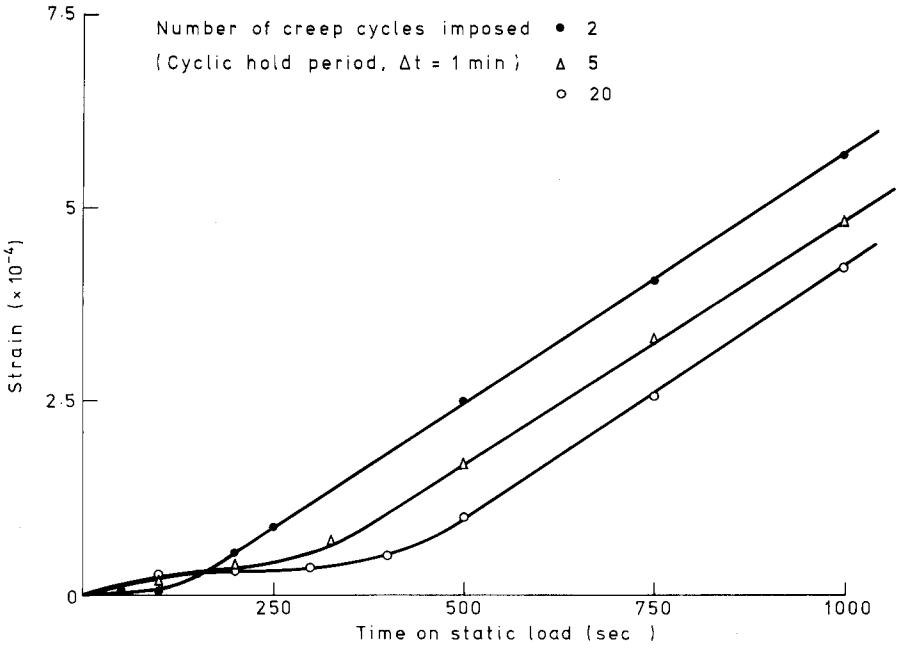


*Figure 8* Creep behaviour on imposing a static load after cyclically loading for a number of cycles at the same frequency ($\Delta t = 1$ min). Load corresponds to an initial stress of 250 MPa.

described in Sections 3.1 and 3.2. There followed a period of decreasing creep rate (illustrated schematically in Fig. 1), and, during cyclic creep testing in the static-to-dynamic creep regime, load removal occurred before the end of this decreasing creep rate period. Imposing a static load after a period of cyclic loading allowed an examination of this transient state and showed that after 5 to 10 min the creep rate increased to the static creep value (see Fig. 7). The results in Fig. 7 also demonstrate that the magnitude of the initial "primary" creep strain and the time before the steady state creep rate was reached both increased with decreasing frequency of prior cycling. Fig. 8 shows the results of a series of tests on statically crept specimens and the effect of imposing a small number of cycles, and finally re-imposing a static load. Both the magnitude of the "primary" creep strain and the time before steady state creep was reached increased with number of cycles, but after approximately 10 cycles there was no further increase.

## 3.6. Microstructural observations

The results of the microstructural observations of internal creep damage are listed in Table II. There were significant changes in damage on cycle loading at fast frequency, notably a generally decreased crack density, with the largest cracks being much shorter and having smaller aspect ratios (length/height). This trend to fewer cracks, with shorter maximum lengths, continued as the frequency of cycling increased.

## 3.7. Square wave cycling

A series of tests carried out using a square wave load cycle indicated that the general behaviour,

TABLE II Microstructural damage parameters after statically and cyclically creep testing to failure. Grain size $50 \times 10^{-6}$ m.

| Testing mode | Applied stress (MPa) | Crack density ($mm^{-2}$) | Maximum crack length ($\times 10^{-6}$ m) | Crack aspect ratio |
|---|---|---|---|---|
| Static | 230 | 80 | 150 | 1.0 |
| | 250 | 80 | 150 | 1.2 |
| | 290 | 50 | 150 | 1.5 |
| Trapezoidal wave; hold period | | | | |
| 6 min | 230 | 70 | 80 | 1.0 |
| 30 sec | 230 | 70 | 60 | 0.8 |
| 6 h | 250 | 80 | 150 | 1.0 |
| 1 h | 250 | 65 | 130 | 1.0 |
| 6 min | 250 | 50 | 60 | 0.8 |
| 30 sec | 250 | 50 | 50 | 0.8 |
| 5 sec | 250 | 50 | 60 | 0.8 |
| 30 sec | 290 | 50 | 70 | 1.5 |

and the influences of stress and frequency, were very similar to those observed with a trapezoidal load cycle. Thus, for example, square wave cycling at low frequency led to large plastic loading increments and reduced rupture lives, while faster cycling led to reduced creep rates and longer rupture lives. Rupture ductility was approximately the same as for static creep, whilst for fast cycling there was a reduction in the intergranular crack density and a decrease in crack size. Thus, the square wave cycling results and behaviour were not significantly different from the trapezoidal cycling data.

## 4. Discussion

### 4.1. Cyclic hardening

Despite the apparent strengthening caused by the cyclic loading suggested in Fig. 3, the observations that the plastic loading increments were dependent only on the unload time prior to reloading, and not on the preceding cyclic history, indicates that no cycling-induced change of structure occurred. The only change observed in thin foils taken from partially crept specimens was an apparent slight decrease in dislocation density during long unloaded periods (~10 h) which was followed by an increase to the original value on reloading. These changes were small, and possibly within the scatter in the dislocation density data. It follows, that no variation in structure leading to cyclic hardening or softening may be invoked to interpret the experimental results.

### 4.2. Anelasticity and dynamic creep

The observation that less anelastic strain recovery occurred in a cyclically creeping specimen than in a statically creeping specimen (Fig. 6) indicates that dislocations within the fast cycled specimens did not take up fully-bowed morphologies. On reloading, the first time-dependent strain was anelastic since unrecoverable creep strain by dislocation link activation cannot accumulate until the dislocation links are almost fully bowed. The partially-bowed nature of dislocation links during cyclic testing may be used to explain the transient loading effects shown in Fig. 7. Since additional recovery of anelastic strain occurred during long unload periods (as in a low frequency test), this resulted in more anelastic strain being re-imposed on loading, and longer times were therefore required for this to occur and unrecoverable creep straining to begin.

According to the present argument, the static-to-dynamic transition may be explained by the very small amount of unrecoverable creep that may occur during the time taken in bowing the

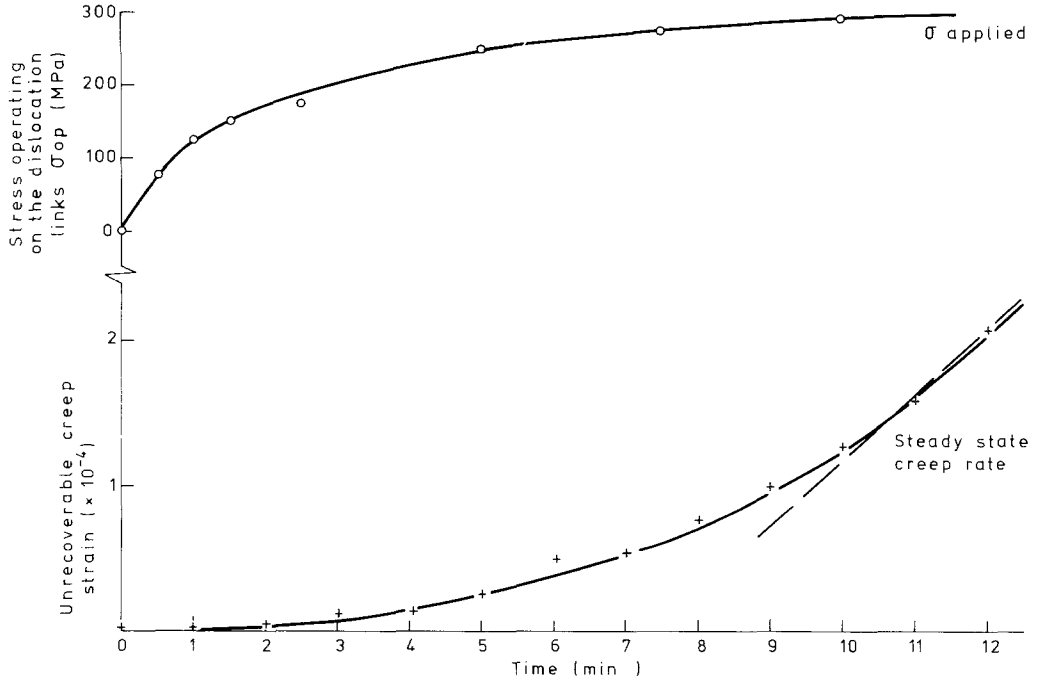


*Figure 9* The variation of the operating stress, $\sigma_{op}$, and the unrecoverable creep strain on reloading after a long period of unloading.

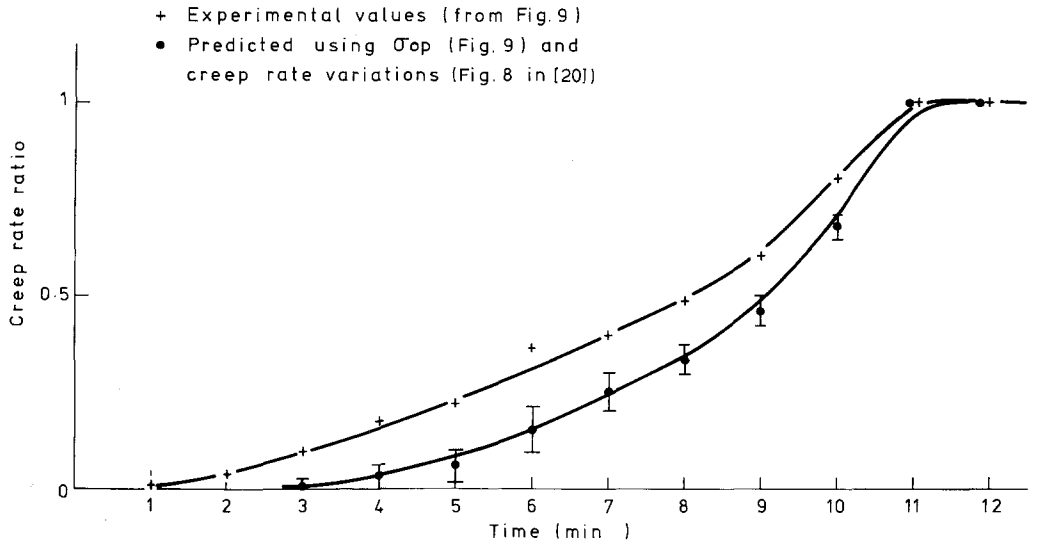


*Figure 10* Comparison of experimental and predicted creep rates during a loading transient.

dislocation links to the fully-bowed state. Thus, the operating stress on the dislocation links, defined as $\sigma_{op} = \mu b/R$, where $\mu$ is the shear modulus, **b** the Burgers vector, and $R$ radius of curvature of the dislocation links, depends on the amount of anelastic strain that has been imposed. The operating stress at any time may be deduced from

$$\sigma_{op}(t)/\sigma_{app} = a(t)/a_{max} \quad (1)$$

where $a(t)$ and $a_{max}$ are the anelastic strain at time $t$ and the maximum that may be imposed at the applied stress, $\sigma_{app}$. Fig. 9 shows the accumulation of unrecoverable creep strain after an unload time of 12 min (that is, the data of Fig. 7 for $\Delta t = 12$ min with the anelastic strain removed) and, also, the increase in the operating stress as the anelastic strain is imposed. Using these operating stress data, together with suitable experimental creep rate–applied stress data (Fig. 8 in [21]), the creep rate at any instant may be calculated and used to predict the total unrecoverable creep strain occurring during a load period of any duration. Fig. 10 shows a comparison of the experimental creep rate ratio (that is the creep strain imposed during a transient of given duration divided by the strain that would accumulate in the same time period during static creep) with values predicted using the approach described. Reasonably good agreement between experiment and theory is demonstrated, indicating the validity of the analytical approach.

Finally, a comparison of static and cyclic creep rates may be made by relating the amount of strain in a given time, $\Delta t$, as a result of creep at the steady state creep rate, $\dot{\epsilon}_s$, to the creep strain imposed during a loading transient of duration $\Delta t$ (using Fig. 9). Table III compares the predicted and experimental (Fig. 6) creep rate ratios (dynamic/static creep rates), where good agreement is again evident.

## 4.3. Damage formation and rupture behaviour

Damage accumulation during the entire lives of specimens is important since the rate of such ac-

TABLE III Comparison of static and dynamic creep rates at 250 MPa.

| Loaded period $\Delta t$ | Strain produced in $\Delta t$ at static creep rate $\Delta\epsilon_s (= \dot{\epsilon}_s \times \Delta t)$ | Strain produced in $\Delta t$ through loading transient $\Delta\epsilon_d$ | Creep rate $\Delta\epsilon_d/\Delta\epsilon_s$ | Experimental creep rate ratio |
|---|---|---|---|---|
| 6 h | $1.4 \times 10^{-2}$ | $1.38 \times 10^{-2}$ | 0.99 | 1 |
| 1 h | $2.3 \times 10^{-3}$ | 1.89 | 0.8 | 1 |
| 6 min | $2.3 \times 10^{-4}$ | $5 \times 10^{-5}$ | 0.22 | 0.24 |
| 30 sec | $2.0 \times 10^{-4}$ | $\sim 10^{-6}$ | $\sim 0.05$ | 0.04 |
| 5 sec | $3.2 \times 10^{-6}$ | $\sim 3 \times 10^{-8}$ | $\sim 0.01$ | $\sim 0.01$ |

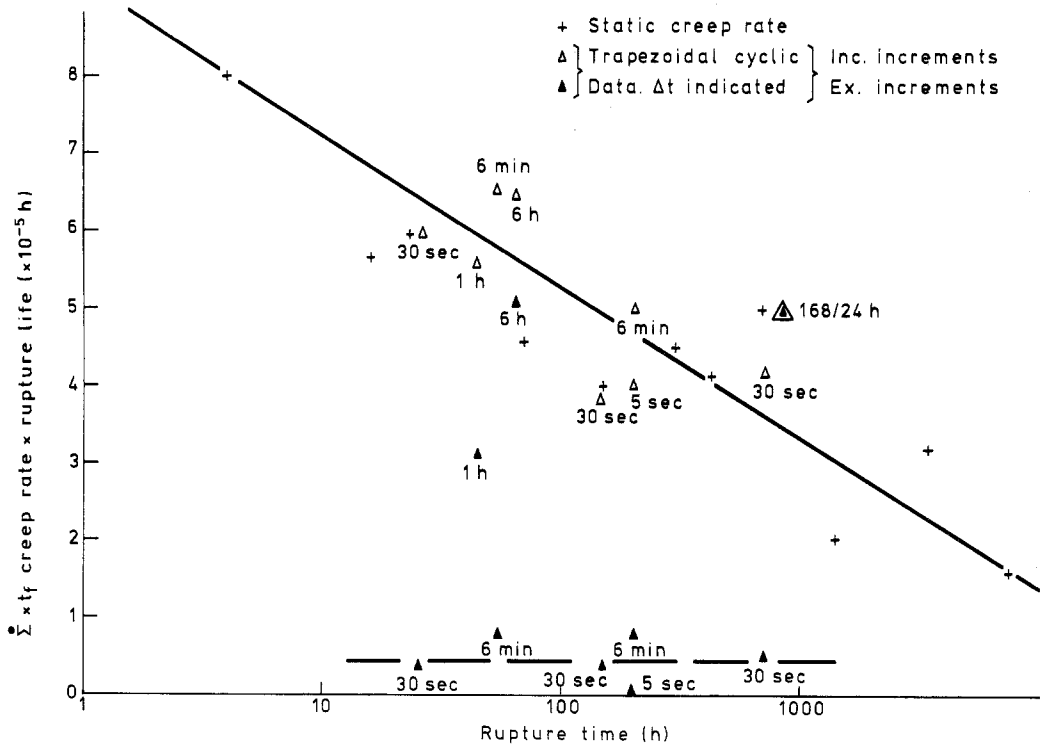


*Figure 11* Minimum creep rate ($\dot{\epsilon}$) multiplied by the rupture time ($t_f$) as a function of rupture time for static and cyclic creep testing.

cumulation determines the crack density and morphology (maximum size, etc.) and it is the material's response to such defects that leads to final failure. The final failure itself is affected by the deformation rate since for faster strains rates there will be less time for stress relaxation and hence smaller defects will be capable of causing failure (see [22] for a discussion of creep failure criteria at similar stresses and temperature).

A comparison of failure under the two testing modes may be made using the $\dot{\epsilon}t_f - t_f$ plot of Fig. 11, together with the ductility and microstructural data. The $\dot{\epsilon}t_f - t_f$ data are very similar for trapezoidal loading (including increments in the creep rate) and for static creep, suggesting that the overall creep during cycling plays much the same role as continuous creep in a static test. It follows that the incremental loading strain is about as damaging as the much slower strain occurring throughout the maximum load periods in the cyclic and during static creep tests. The slightly increased ductility and reduced crack density observed for higher frequency cycling suggest that the incremental loading strain is actually slightly less damaging than the slower creep strain. The reduced maximum crack length under such conditions is a result of the reduced crack density, since it appears that crack growth occurs by the linkage of randomly nucleated cracks in this material [22]. Consequently somewhat larger ductilities and higher stresses are imposed during rapid cycling before failure occurs.

## 5. Conclusions

(1) The strain imposed during cyclic creep testing occurs in the form of very rapid strain increments produced on loading and much slower creep strain during the maximum load periods.

(2) The incremental strain depends only on dislocation recovery during the unload period with no evidence of a cyclically produced structural change. Unrecoverable creep strain can occur only when dislocations have become almost fully bowed as the anelastic strain is imposed. The static-to-dynamic transition accordingly occurs when cycling at high frequencies such that significant anelastic strain is never imposed during the maximum load part of the cycle.

(3) Failure over the range of cyclic loading conditions examined here occurs by static creep rupture mechanisms, namely the nucleation and

growth of wedge cracks leading to final rapid failure when sufficiently long cracks have formed.

(4) All the strain imposed during cyclic creep (both the rapid loading strain and the much slower creep strain) leads to intergranular crack damage. The rapid incremental strain appears to be slightly less damaging than the slow creep strain such that higher ductilities are achieved in high frequency cyclic tests where most of the strain is imposed as rapid incremental strain.

## References


1. Symposium on the effect of cyclic heating and stressing on metals at elevated temperatures, ASTM STP No. 165 (1954).
2. R. ROTERAZAWA and T. SHIMOHATA, International Conference on Creep and Fatigue in Elevated Temperature Applications, Sheffield, 1974, p. 214. 1.
3. R. KOTERAZAWA, Proceedings of the 14th Japanese Congress on Materials Research, 1971, p. 73.
4. *Idem,* Proceedings on the International Conference on Mechanical Behaviour of Metals, 1972, Vol. III, p. 135.
5. B. J. LAZAN, *Proc. Amer. Soc. Test. Mater.* 49 (1949) 757.
6. B. J. LAZAN and E. WESTBERG, *ibid* 52 (1952) 837.
7. L. A. YERKOVICH and G. J. GUARNIERI, WADC TR5S-226 (1955).
8. F. H. VITOVEC, *Proc. Amer. Soc. Test. Mater.* 57 (1957) 977.
9. D. SHETTY and M. KOSHII, International Conference on Creep and Fatigue in Elevated Temperature Applications, Sheffield, 1974, p. 188. 1.
10. C. E. FELTNER and G. M. SINCLAIR, Joint International Conference on Creep, Proceedings of the Institute of Mechanical Engineers, 175 (1963) 3.
11. J. T. EVANS and R. N. PARKINS, *Acta Met.* 24 (1976) 511.
12. J. N. GREENWOOD, *J. Proc. Amer. Soc. Test. Mater.* 49 (1949) 834.
13. A. J. KENNEDY, Proceedings of the International Conference on the Fatigue of Metals (Institute of Mechanical Engineers, London, 1956) p. 401.
14. A. H. MELEKA and A. V. EVERSHED, *J. Inst. Metals* 88 (1959) 411.
15. M. F. DAY and W. M. CUMMINGS, *J. Mech. Eng. Sci.* 10 (1968) 36.
16. L. H. TOFT and T. BROOM, Proceedings of the Institute of Mechanical Engineers 179 3A (1963) 77.
17. S. TAIRA, M. OHNAMI and M. SAKATO, *Bull. JSME* 5 (1962) 17.
18. G. F. HARRISON and G. P. TILLEY, International Conference on Creep and Fatigue in Elevated Temperature Applications, Sheffield, 1974, p. 173.
19. E. G. ELLISON and D. WALTON, *ibid* p. 173.
20. D. G. MORRIS and D. R. HARRIES, *J. Mater. Sci.* 12 (1977) 1587.
21. D. G. MORRIS, *Acta Met.* (to be published).
22. *Idem, Metal. Sci.* (to be published).


Received 5 July and accepted 21 September 1977.